Computational Studies on Optoelectronic and Nonlinear Properties of Octaphyrin Derivatives

Nasarul Islam[1]* and Irfan H. Lone[2]

[1] *Department of Chemistry, Guru Nanak Dev University, Amritsar, India,* [2] *Department of Chemistry, Government Degree College, Kupwara, India*

The electronic and nonlinear optical (NLO) properties of octaphyrin derivatives were studied by employing the DFT/TDFT at CAM-B3LYP/6-311++G (2d, 2p) level of the theory. Thiophene, phenyl, methyl and cyano moieties were substituted on the molecular framework of octaphyrin core, in order to observe the change in optoelectronic and nonlinear response of these systems. The frontier molecular orbital studies and values of electron affinity reveals that the studied compounds are stable against the oxygen and moisture present in air. The calculated ionization energies, adiabatic electron affinity and reorganization energy values indicate that octaphyrin derivatives can be employed as effective n-type material for Organic Light Emitting Diodes (OLEDs). This character shows an enhancement with the introduction of an electron withdrawing group in the octaphyrin framework. The polarizability and hyperpolarizability values of octaphyrin derivatives demonstrate that they are good candidates for NLO devices. The nonlinear response of these systems shows enhancement on the introduction of electron donating groups on octaphyrin moiety. However, these claims needs further experimental verification.

Keywords: porphyrin, reorganization energy, bond-length-alternation, mesomeric effect, polarizability, hyperpolarizability

INTRODUCTION

The discovery of sapphyrins and expanded porphyrins have attracted the interest of researchers attributed to their diverse applications in materials science (Sprutta and Latos-Grazyński, 2001; Flemming and Dolphin, 2002; Pushpan et al., 2002; Silva et al., 2002a,b; Cavaleiro et al., 2003; Hata et al., 2006; Tanaka and Osuka, 2016). The defining feature of these macrocycles is the presence of a larger internal cavity as compared to those present in natural tetrapyrroles. More specifically, expanded porphyrins are macrocyclic compounds containing five-membered heterocyclic units (like pyrrole, furan, or thiophene) linked together, either directly or through spacers with internal ring pathway contains at least 17 atoms (Sprutta and Latos-Grazyński, 2001; Flemming and Dolphin, 2002; Pushpan et al., 2002; Silva et al., 2002a,b; Hata et al., 2006). Their distinctive physical and structural properties have found applications in nonlinear optical (NLO) materials (Marder et al., 1997; Zhou et al., 2002; Ahn et al., 2005; Rath et al., 2005a; Misra et al., 2006), photosensitizers for photodynamic therapy (PDT) (Harriman et al., 1989; Maiya et al., 1989), transition or rare earth metal ion chelates, cation and anion receptors (Shionoya et al., 1992; Jasat and Dolphin, 1997; Sessler et al., 2000a,b; Sessler and Davis, 2001; Chandrashekar and Venkatraman, 2003), magnetic resonance imaging (MRI) contrasting agents (Charrière et al., 1993; Weghorn et al., 1996; Werner et al., 1999) and a tool for accessing presently unknown higher aromatic systems

Graphical Abstract
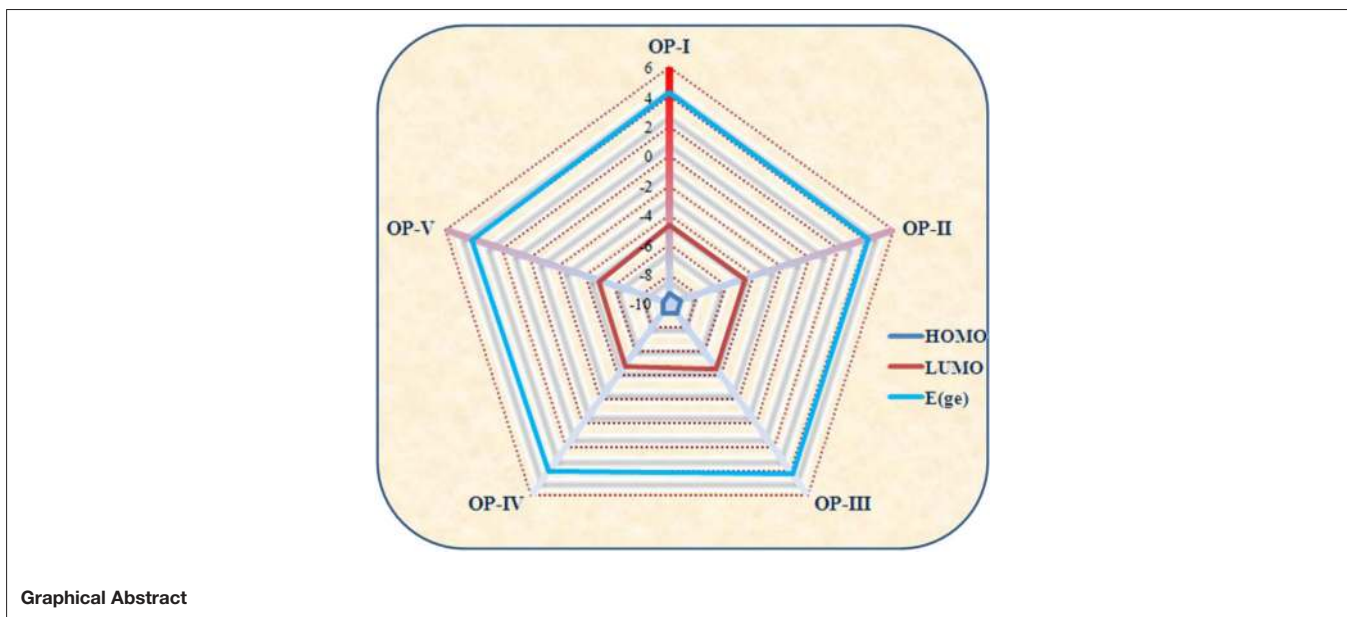
(Sessler et al., 1993). These fascinating properties have inspired synthetic efforts toward a range of expanded porphyrins differing in ring size, ring connectivity, peripheral substituent and core modification (Hiroto et al., 2006; Misra and Chandrashekar, 2008; Anaka et al., 2011; Mori et al., 2012a; Kido et al., 2013; Naoda and Osuka, 2014; Anguera et al., 2015). These modifications not solely amendment their electronic properties, but also conjointly create structural diversity to induce ring inversion in the resulting macrocycles. Currently, considerable attention has been focused on the studies of organic molecules capable of exhibiting organic light emitting properties or massive NLO susceptibilities. Researchers have observed that the presence of extended π-electron delocalization is the key element in the design of organic molecules exhibiting either the OLED or NLO applications (Geffroy et al., 2006; Sasabe and Kido, 2011, 2013a,b; Jin and Tang, 2013; Sekine et al., 2014; Islam and Pandith, 2014a; Romain et al., 2015).

The expanded porphyrins that display the greatest resemblance to natural porphyrins are those containing either meso-like bridging carbon atoms or direct links between the heterocyclic subunits. According to the nomenclature put forward by Franck and Nonn (Franck and Nonn, 1995), the name of these systems consists of three parts: (1) the number of π-electrons in the shortest conjugation pathway (in square brackets), (2) a core name indicating the number of pyrroles or other heterocycles (e.g., pentaphyrin, hexaphyrin), and (3) the number of bridging carbon atoms between each pyrrole subunit (in round brackets and separated by dots). For instance, according to this nomenclature, the classic porphyrin macrocycle presented in the heme group would be named as [18] tetraphyrin (1.1.1.1). Octaphyrin (1.1.1.1.1.1.0.0) (**OP**), being a conjugated π system may be the excellent candidate for the materials science. Many research groups have reported the synthesis and structural properties of isomers of Octaphyrin (1.1.1.1.1.1.0.0)

(Franck and Nonn, 1995; Latos-Grazynski, 2004; Shimizu et al., 2005; Rath et al., 2005b; Geffroy et al., 2006; Hiroto et al., 2006; Kumar et al., 2007; Misra and Chandrashekar, 2008; Anaka et al., 2011; Sasabe and Kido, 2011, 2013a,b; Mori et al., 2012a; Jin and Tang, 2013; Kido et al., 2013; Naoda and Osuka, 2014; Sekine et al., 2014; Islam and Pandith, 2014a; Anguera et al., 2015; Romain et al., 2015). According to Chandershaker et al. the core-modified expanded porphyrins containing 26, 36, and 54 π electrons because of their exceptionally massive two-photon absorption cross- sections may be considered among the most effective appropriate candidates, particularly as organic NLO materials (Pushpan and Chandrashekar, 2002). The derivatives of hexaphyrins and octaphyrins containing meso-imidazolyl groups were prepared by research group of Hirotaka et al. (Mori et al., 2012b). They found that hydrogen bonding is effective for the development of Huckel antiaromatic expanded porphyrins. The molecular framework of octaphyrin is consistent with a 36 π-electron circuit within what can be considered a twisted double-side (orientable) Huckel topology (Sprutta and Latos-Grazyński, 2001; Flemming and Dolphin, 2002; Pushpan et al., 2002; Silva et al., 2002a,b; Hata et al., 2006). According to Osuka et al. the hydrogens present near the crossing point of the octaphyrin resonate at δ = 17.14 and 8.60 ppm in the deshielding region. These findings are consistent with the presence of paratropic ring current and categorizing the octaphyrin among the Huckel type antiaromatic system. Various studies were performed for explaining the conformational switch between Hückel planar and Möbius twisted topologies of expanded porphyrins (Torrent-Sucarrat et al., 2012; Alonso et al., 2013, 2014; Marcos et al., 2014). Observations revealed that the nature of the meso-substituent is important for determining the relative stability of the Hückel−Möbius conformers and interconversion also between them is controlled by the barrier height (Torrent-Sucarrat et al., 2012; Marcos et al., 2014). Proft

et al. employed DFT at B3LYP/6-31G (d,p) level of theory to study the conformational preferences, interconversion pathways and aromaticity of N-fused [22] and [24] pentaphyrins. They have observed that the choice of conformation strongly depend upon the oxidation state, aromaticity of the π-electron system and meso-substituents (Alonso et al., 2013, 2014).

Conjugated organic systems are principally explored as hole transport materials for the organic light emitting devices (Fink et al., 1998; Jurchescu et al., 2004; Park et al., 2011; Tao et al., 2011; Kim et al., 2013; Wu et al., 2014; Islam and Pandith, 2014b; Fan et al., 2015). Because of troublesome processsbility and instability in air, the exploration, design and synthesis of electron transport material has remained a significant challenge and hot stock within the field of organic electronics (Pandith and Islam, 2014; Zhao et al., 2014). Within the recent years, conjugated nitrogen containing organic derivatives have been found as promising n-type or p-type materials for the fabrication of OLED (Fink et al., 1998; Jurchescu et al., 2004; Park et al., 2011; Tao et al., 2011; Kim et al., 2013; Pandith and Islam, 2014; Wu et al., 2014; Zhao et al., 2014; Islam and Pandith, 2014b; Fan et al., 2015). The material acquires this property because of their excellent optoelectronic properties, good oxidation and thermal stabilities, large electron affinities and high electron mobilities. In the first section of paper, we have studied optoelectronic properties of octaphyrin derivatives (**OP**) (**Figure 1**) to explore their potential as n-type material for OLED devices and have calculated their reorganization energies, ionization potentials and electron affinity values. In the second section we have explored the octaphyrin derivatives as a class of organic molecules suitable for NLO applications.

A significant interest still exists for novel molecular materials with optimal NLO properties because of their primary roles in applications in fields including optical communications and computation, optical switching and limiting, data storage and retrieval, and sensors (Islam et al., 2014; Dadsetani and Omidi, 2015). The nonlinear response of molecules to electromagnetic fields has been studied over the last two decades. It provides a way for amplification, modulation and changing the frequency of optical signals (Liu et al., 2011; Lin et al., 2015). Materials with massive hyperpolarizabilities have found applications in optoelectronics, such as optical switching for optical computing or high-density optical recording. Several experimental and theoretical studies have been administrated to identify materials with large hyperpolarizabilities (Datta and Pati, 2006; Lakshmi et al., 2008; Lin et al., 2013; Rintoul et al., 2013; Dai et al., 2014; Liu et al., 2014; Islam and Chimni, 2017). As a result of distinctive structure octaphyrins with extended π electrons can prove smart candidates for NLO response. So as to visualize its optical properties, we have calculated the polarizability (α), the first-order hyperpolarizability (β) and also the second-order hyperpolarizability (γ) of octaphyrin. According to Dai et al. (2014); Rintoul et al. (2013); Lin et al. (2013); Liu et al. (2014), Datta and Pati (2006), Lakshmi et al. (2008) and Islam and Chimni (2017) second-order response governed by the second order hyperpolarizability offers more varied and richer behavior than first-order NLO process due to the higher dimensionality of the frequency space. Therefore, we have also calculated the second-order hyperpolarizability of the octaphyrin derivatives, in order to conclude their appropriate NLO response.

COMPUTATIONAL STUDIES

In the present study, structural and optoelectronic calculations of **OP** derivatives were performed by using Density functional theory. The geometries were optimized by employing CAM-B3LYP (Yanai et al., 2004) functional using 6-31G (2d, 2p) (Ditchfield et al., 1971), and 6-311++G (2d, 2p) (McLean and Chandler, 1980) basis sets. Frequency calculations at the same level of theory were performed to confirm each stationary point to be a true energy minimum. The neutral molecules were treated as closed-shell systems, while for the radical anion or cation open-shell system optimizations were carried out using a spin unrestricted wave functional. The parameters governing the NLO properties calculated at CAM-B3LYP functional were found comparble more accurate in the previous studies (Torrent-Sucarrat et al., 2011). The electronic absorption spectra of **OP** derivatives were calculated at TD-DFT/CAM-B3LYP/6-311++G (2d, 2p) level of theory. The calculation for the lowest transition was derived from the Gaussian output file using the GaussSum program (O'Boyle et al., 2008). All the calculations were performed using the Gaussian 09 computational package (Frisch et al., 2009).

RESULTS AND DISCUSSION

The optimized geometries of **OP** derivatives obtained from DFT calculations are illustrated in **Figure 2**. These systems exist in two atropisomeric forms *P* and *M* (Sprutta and Latos-Grazyński, 2001; Flemming and Dolphin, 2002; Pushpan et al., 2002; Silva et al., 2002a,b; Cavaleiro et al., 2003; Hata et al., 2006; Tanaka and Osuka, 2016). *P* and *M* isomeric forms are the mirrors images of each other, which do not show any distinction in electronic properties. The assignment of atropisomeric forms depends on the sense of the helical twist, it could be clockwise and denoted by **P** ("plus") for a right-handed helix or be anticlockwise and denoted by **M** ("minus") for a left-handed helix. In this study *P*-isomer was considered for the evaluation of electronic and optical properties. Computational calculations display that all the studied **OP** geometries vary in the orientation of pyrrole rings and the two centers, each containing four pyrrole rings, are coplanar to each other. In **OP-I** pyrrole rings are oriented in such a manner that all the nitrogen groups are toward the center (core) of molecule. In case of **OP-II** and **OP-III** the methyl and the phenyl groups present on C_{24} and C_{32} are oriented toward the center (core) resulting in hyperbolic nonlinearity in the derivatives respectively. However, in case of **OP-IV** the pyrrole ring D and B are oriented away from the center, resulting in chair type geometry of the derivatives. The thiophene rings remain away from core and point toward the corner position of the three dimensional box in **OP-IV** derivative. Cyano group being linear, thus the geometry of **OP-V** does not vary abundantly from **OP-I**. In addition, cyano groups are directed alternatively away and toward the center of octaphyrin segment. Comparing
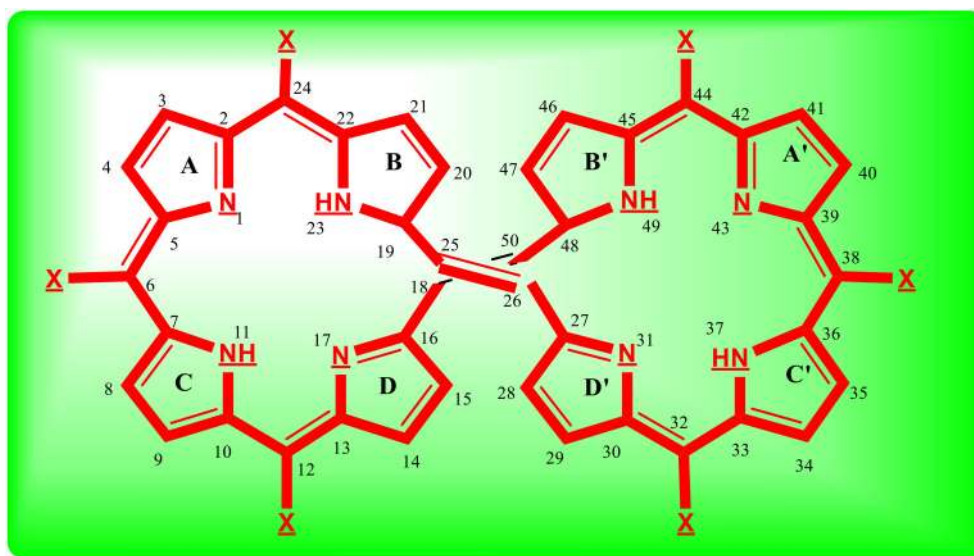
FIGURE 1 | Sketch of octaphyrin (OP) derivatives study using DFT at CAM-B3LYP/6-311++G (2d, 2p) level of theory.

the bond length of the **OP** derivatives, the C_{16}-C_{18} bond is shorter in case of **OP-V** as compared to OP-I following the trend OP-V < OP-IV < OP-III < OP-II = OP-I. On the other hand the bond length of $C_{18} = C_{26}$ within derivatives is longer just in case of **OP-V** as compared to **OP-I**. The decrease in the C_{16}-C_{18} bond length shows some double bond character, which suggests that upon substitution with cyano group the π electron delocalization is enhanced over the entire frame work instead of localized between the particular nuclei. Thus, electron delocalization leads to the change in bond length or polarization in these systems. The impact of substitution on the aromaticity and charge transfer was analyzed by calculating the bond length alternation (**BLA**) values. Bond length alternation is a construct that can be used to monitor the amount of change in polarization across the bonds in a molecule upon substitution. Fu et al. (2008) defined BLA as the average of the difference in the length between adjacent carbon-carbon bonds in a polymethine $[(CH)_n]$ chain. In this work we calculated a local BLA associated with the C_{16}-C_{18}, $C_{18} = C_{26}$ and C_{26}-C_{48} bond lengths and consistent with the definition given by Fu et al., BLA is given as:

$$BLA = \frac{d(C_{16} - C_{18}) + d(C_{26} - C_{48})}{2} - d(C_{18} = C_{26}) \quad (1)$$

The BLA values obtained from the above equation follow the trend OP-V (0.261) < OP-III (0.297) < OP-II (0.306) < OP-IV (0.310) < OP-I (0.312). Thus, the substitution of hydrogen atom with electron withdrawing groups (cyano here) has less effect on

the geometry of **OP**. The OP-I displays higher value followed by OP-II, OP-III and OP-IV indicating that the presence of methyl, phenyl and thiophene substituents have a scarce influence on the aromaticity of the series of studied compounds.

OLED Properties

The charge transfer properties play a vital role in high performance OLED devices. Charge transfer within the materials is often viewed in light of two headings, i.e., hopping theory (Lin et al., 2003) and the band theory (Cheng et al., 2003). Under the frame of hopping theory, the charge carrier is absolutely localized on a single molecule for the limit of thermal disorder and therefore the charge transfer happens between small coupled neighboring molecules. However, according to the band theory transport of charge is an activationless process, occurring through bands fashioned by the overlapping MOs between neighboring molecules. Under the heading of the hopping model the rate of charge transfer is described by the standard Marcus electron-transfer theory. According to Marcus the rate of electron or hole-transfer k_{et} is given by the following equation (Marcus, 1957a,b).

$$k_{et} = \left(\frac{4\pi^2}{h}\right) \Delta H_{ab}^2 (4\pi \lambda k_B T)^{-\frac{1}{2}} \exp\left(\frac{-(\Delta G^0 + \lambda)^2}{4\lambda k_B T}\right)$$
$$(2)$$

were λ and ΔH_{ab} are the reorganization energy for the intramolecular electron transfer and the electronic coupling integral between donor-acceptor pair, respectively, and ΔG^0 is

FIGURE 2 | Optimized geometries of OP derivatives obtained at CAM-B3LYP/6-311++G (2d, 2p) level of calculations.
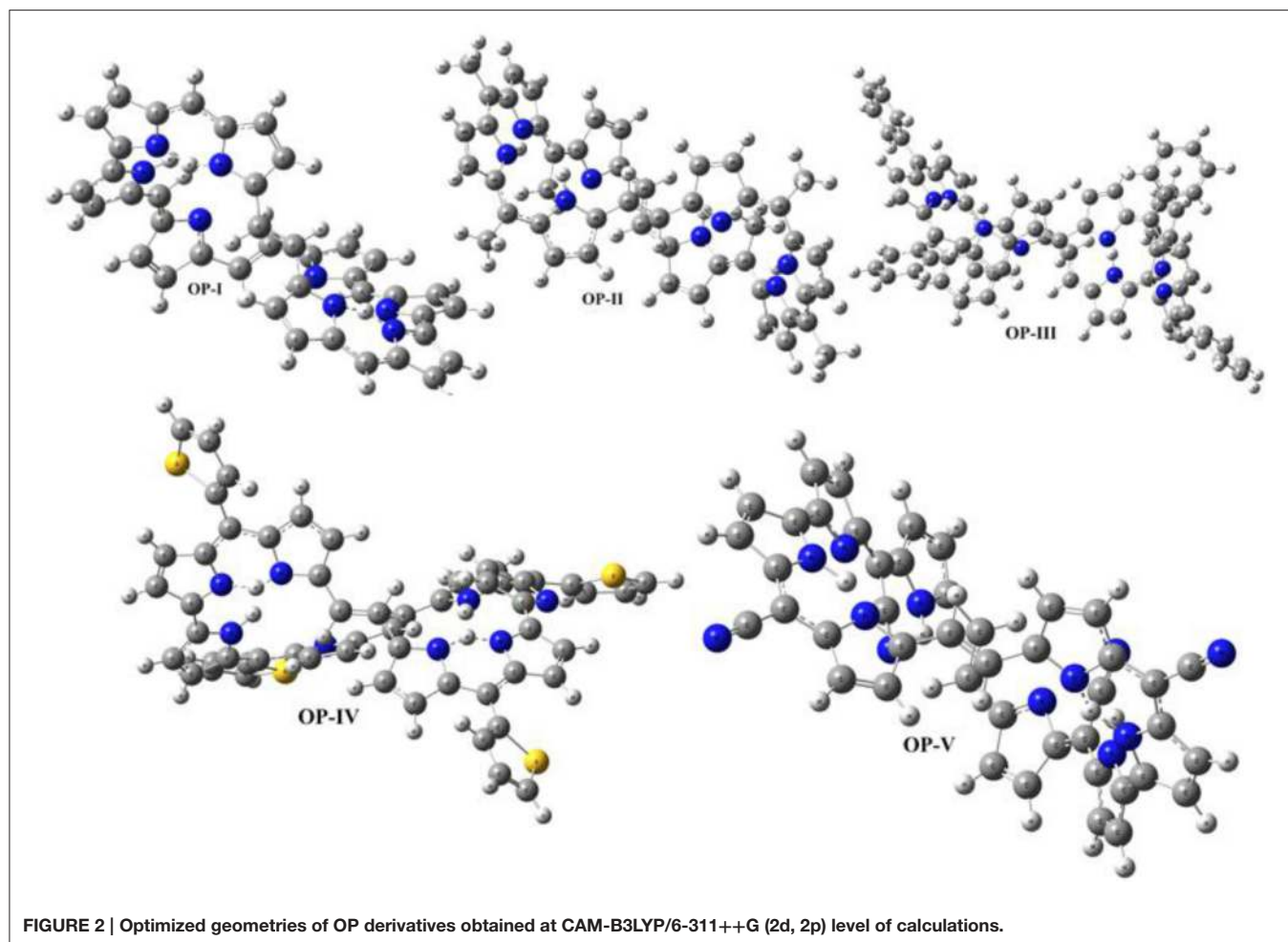
TABLE 1 | Ionization energy, adiabatic energy, and reorganization energy of OP derivatives calculated by employing DFT/CAM-B3LYP/6-311++G (2d, 2p) level of theory.

	IP$_{adiabatic}$ (eV)	IP$_{vertical}$ (eV)	EA$_{adiabatic}$ (eV)	EA$_{vertical}$ (eV)	λ_{hole} (eV)	$\lambda_{electron}$ (eV)
OP-I	6.82	6.89	3.09	3.13	0.211	0.131
OP-II	6.87	6.93	3.32	3.33	0.209	0.129
OP-III	6.92	6.96	3.41	3.49	0.221	0.124
OP-IV	6.98	7.01	3.53	3.51	0.228	0.121
OP-V	7.04	7.12	3.61	3.63	0.217	0.118

Were IP$_{adiabatic}$ is adiabatic ionization potential, IP$_{vertical}$ vertical ionization potential, EA$_{adiabatic}$ adiabatic electron affinity, EA$_{vertical}$ vertical electron affinity, λ_{hole} and $\lambda_{electron}$ reorganization energy for hole and electron transport respectively.

the Gibbs free energy change of the process. The reorganization energy includes the contributions from the intramolecular and intermolecular energy change during a charge transfer event. The intramolecular reorganization energy refers to the relaxation of the molecule involved in the charge transfer process and the intermolecular reorganization energy refers to the relaxation of the medium in which the charge transfer takes place. From Equation (2) it is clear that λ be low to get a high electron or hole transfer rate. Various studies have defined that first-principles quantum chemistry calculations would be productive

to investigate the charge transport properties. In this study we have focused on estimating the intramolecular reorganization energy (λ) to evaluate the optoelectronic properties of studied molecule. So, the reorganization energies for the hole and electron transfers are evaluated using the following formulas (Tavernier and Fayer, 2000).

$$\lambda_h = \left[E\left(M^+\right)\right] - \left[E\left(M\right)\right] + \left[E^+\left(M\right) - E^+\left(M^+\right)\right] \quad (3)$$
$$\lambda_e = \left[E\left(M^-\right)\right] - \left[E\left(M\right)\right] + \left[E^-\left(M\right) - E^-\left(M^-\right)\right] \quad (4)$$

TABLE 2 | FMO (HOMO and LUMO energies) and Optical data of OP derivatives calculated by employing DFT and TDFT level of theory respectively.

	HOMO (eV)	LUMO (eV)	ΔE	λ_{max}	E_{ge}	f	Orbital contribution
OP-I	−9.2622	−4.603	4.659	530	4.341	0.722	HOMO → LUMO 81 %
OP-II	−9.1713	−4.611	4.560	538	4.217	0.718	HOMO → LUMO 69 %
OP-III	−9.2099	−4.628	4.582	540	4.202	0.701	HOMO → LUMO 78 %
OP-IV	−9.2326	−4.819	4.414	612	4.001	1.015	HOMO → LUMO 95 %
OP-V	−9.5175	−4.986	4.532	526	4.112	0.855	HOMO → LUMO 90 %

Were HOMO is highest occupied molecular orbital energy, LUMO lowest unoccupied molecular orbital energy, ΔE energy gap between HOMO and LUMO, λ_{max} maximum absorption wavelength, E_{ge} excitation energy and f oscillator strength corresponding to S_0 to S_1 excitation.

where $E(M)$, $E^+(M^+)$, and $E^-(M^-)$ are the respective energies of optimized neutral, cationic, and anionic structures. $E(M^+)/E(M^-)$ is the neutral energy of the optimized cationic/anionic structure, and $E^+(M)/E^-(M)$ is the cationic/anionic energy of the optimized neutral structure. The calculated values of intramolecular reorganization energies for **OP** derivatives are given in **Table 1**. We have observed that λ_e (reorganization energy for electron transport) values are comparatively smaller as compared to the λ_h (reorganization energy for hole-transport) values demonstrating relevance of studied **OP** derivatives as n-type material for Organic Light Emitting devices. However, upon derivatization the value of λ_e further decreases and is a minimum for **OP-V** containing CN-groups. The λ_e values obtained for OP derivatives were found smaller as compared to reported compounds projected as economical n-type candidates for OLED devices (Pandith and Islam, 2014; Zhao et al., 2014; Naka et al., 2000). According to Liu et al. (2010) the ionization potential (IP) together with the electron affinity (EA) can be used to weigh the hole and electron injection properties respectively. The vertical and adiabatic ionization potential and electronic affinity of OP derivates were calculated by using the following equations and are given in **Table 1**.

$$IP(v)/IP(a) = E^+(M)/E^+(M^+) - E(M) \qquad (5)$$

$$EA(v)/EA(a) = E(M) - E^-(M)/E^-(M^-) \qquad (6)$$

Where $IP(v)/IP(a)$ and $EA(v)/EA(a)$ are vertical and adiabatic ionization potential and electron affinity respectively. The calculated EA values for the OP derivatives are all greater than 3.00 eV defining their anionic stability toward the oxygen present in surrounding. Based on the recent theoretical studies EA for air stable n-type material should be greater than 2.80 eV (Newman et al., 2004; Chang et al., 2010). Thus, according to these observations the studied compounds are quite stable to moisture present in air as n-type material on account of their large adiabatic electron affinity values. On the basis of above calculations, the electron affinity values of OP derivatives follow the trend OP-I < OP-II < OP-III < OP-IV < OP-V (**Table 1**). The OP-V scores maximum EA and IP value; therefore in case of OP-V the holes and electrons can be consequently injected into the emissive layer much more easily. Thus, combining the relationships between charge injection and the values of EA, it is concluded that the electron injection properties are improved with the introduction of electron withdrawing groups.

All the studied octaphyrins exhibit π-character that spreads over the entire molecule resulting in delocalization, demonstrating their efficient charge transfer ability. The theoretical calculation shows that these molecules have low lying HOMO and LUMO energy levels that signifies that they possess high oxidation and reduction stabilities. As seen from **Table 2** the LUMO of the OP derivatives reaches from −4.6 to −4.9 with the substitution. On relating our findings with the calculations carried by Usta et al., the studied OP can be applicable with the work function of the metal electrode like Au (−5.1 eV) and Pt (−5.6 eV) used in practical OFET devices (Usta et al., 2009). It has been observed that the electron injection potential barrier for n-type material between the OP and metal electrode decreases with the introduction of an electron withdrawing group on OP skeleton. The frontier molecular orbital analysis (**Figure 3**) displays the change in HOMO-LUMO distribution over the OP framework initiated either by mesomeric or inductive effect. The former has relevance to the sharing of π-electrons between the parent and substituents whereas the latter is expounded to the σ−electron systems.

For the above system the LUMO energies decrease both with electron donating as well as electron withdrawing substituents and attributable to different decreasing degrees in HOMO and LUMO the energy gaps for these OP derivatives become distinguishable. Analyzing the energy gap between the HOMO and LUMO, the **OP-IV** displays the lowest value and **OP-I** the highest value. Thus, the potency of OP derivatives as n-type material as per the values of EA and λ_e does not correlate well with the energy gap between HOMO and LUMO. The frontier molecular orbital (FMO) studies reveal that the highest occupied molecular orbitals (HOMOs) of the neutral molecules delocalize primarily over the octaphyrin skeleton with least contribution from the substituents, whereas the lowest unoccupied molecular orbitals (LUMOs) have an obvious electron density distribution including contribution from Octaphyrin skeleton and as well as from substituents. These orbital pictures defines that the energy levels of the LUMOs rather than that of HOMOs are more affected by the introduction of the substituent moiety. The TD-DFT studies at CAM-B3LYP/6-311++G (2d, 2p) level of theory reveal that in all octaphyrin moieties the absorption spectra display a single peak with slight red shift in case of cyano group and remarkable blue shift in case of OP-IV. From **Table 2**, the primary excited state (S1) of **OP** derivatives originates from the HOMO to LUMO transitions with contributions of about 95 and 69% in case OP-IV and OP-II respectively. Thus, on the
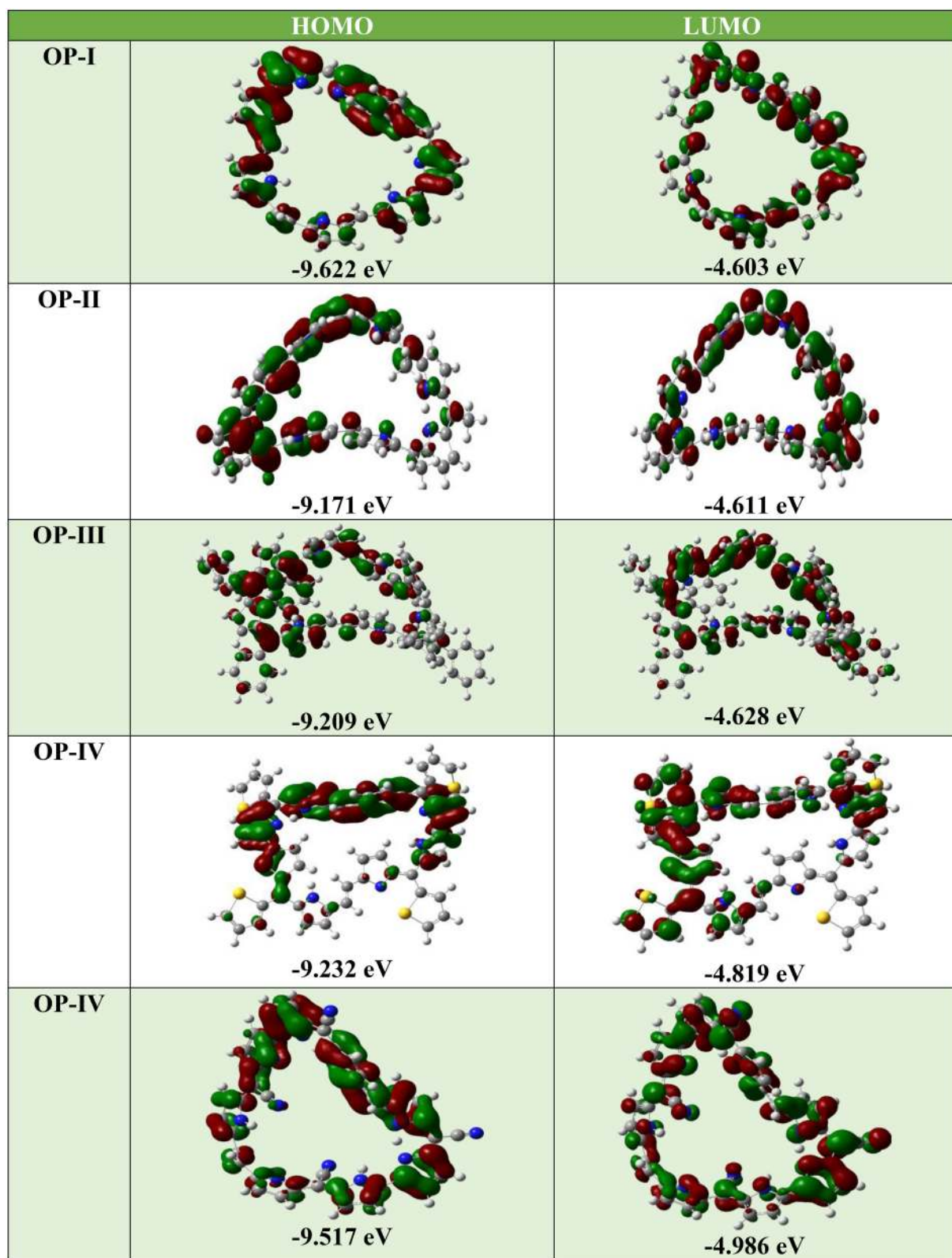
HOMO	LUMO
OP-I −9.622 eV	−4.603 eV
OP-II −9.171 eV	−4.611 eV
OP-III −9.209 eV	−4.628 eV
OP-IV −9.232 eV	−4.819 eV
OP-IV −9.517 eV	−4.986 eV

FIGURE 3 | The frontier molecular orbitals (FMOs) of OP derivatives at DFT/ CAM-B3LYP/6-311++G (2d, 2p) level of theory.

TABLE 3 | DFT/TDFT calculated average values of the dipole moment (in ground (μ_{gg}) and excited state (μ_{ee}), transitions dipole moment (μ_{ge}^2), static polarizability α (Å^3), the first polarizability β (esu.) and the second polarizability γ (esu) for OP derivatives.

	μ_{gg}	α (×10^{-23})	β (×10^{-33})	γ (×10^{-35})	μ_{ee}	μ_{ge}^2	μ_{ge}^2 / E_{ge}^2
OP-I	3.80	93.98	2,086.31	−3353.42	3.92	0.94	0.048
OP-II	4.54	144.29	7,906.63	−2196.50	4.69	0.99	0.056
OP-III	4.91	157.20	7,911.70	−1686.21	5.18	1.01	0.057
OP-IV	5.37	203.23	10,349.22	445.33	6.81	1.15	0.072
OP-V	3.98	111.50	4,038.53	−2122.97	4.51	1.08	0.063

basis of above calculations we will conclude that OPs sustain position as an optoelectronic material, however, by introducing electron withdrawing groups they will prove as an effective n-type material for OLEDs.

Nonlinear Optical Response

Octaphyrin being a conjugated pathway can become a potential material for NLO response. NLO techniques are considered as among the most structure-sensitive methods to study the molecular structures and assemblies. Quantum chemical calculations are shown to be useful within the description of the relationship among the electronic structure of these systems and their NLO response. During this study, the dipole moment, polarizability and first-order hyperpolarizability and second order hyperpolarizability were used to evaluate the nonlinear response of Octaphyrin derivatives. The average linear polarizability <α>, first order hyperpolarizability < β > and second order hyperpolarizability < γ> values have been calculated from Gaussian output file using the following relations.

The microscopic polarizability (P) induced in an isolated molecule under the applied electric field (E) of an incident electromagnetic wave can be expressed by the following equation:

$$P = \alpha_E + \beta_{EE} \qquad (7)$$

Where P and E are related to the tensor quantities α and β which are referred to as the polarizability and hyperpolarizability, respectively.

The definition (Sajan et al., 2006; Alyar et al., 2007; Sundaraganesan et al., 2009; Zhang et al., 2010) for the polarizability is:

$$\langle \alpha \rangle = {}^1/_3 \; (\alpha_{xx} + \alpha_{yy} + \alpha_{zz}) \qquad (8)$$

The anisotropy of polarizability is:

$$\Delta \alpha = 1/\sqrt{2} \Big[(\alpha_{xx} - \alpha_{yy})^2 + (\alpha_{yy} - \alpha_{zz})^2 + (\alpha_{zz} - \alpha_{xx})^2$$
$$+ 6\alpha_{xz}^2 + 6\alpha_{xy}^2 + 6\alpha_{yz}^2 \Big]^{1/2} \qquad (9)$$

And the first hyperpolarizability is a third rank tensor that can be described by a 3 × 3 × 3 matrix (Thanthiriwatte and de Silva,

2002). The components of can β be calculated using the following equation:

$$\langle \beta \rangle = \Big[(\beta_{xxx} + \beta_{xyy} + \beta_{xzz})^2 + (\beta_{yyy} + \beta_{yzz} + \beta_{yxx})^2$$
$$+ (\beta_{zzz} + \beta_{zxx} + \beta_{xyy})^2 \Big]^{1/2} \qquad (10)$$

or simply:

$$\beta_{\parallel} = \frac{1}{5} \sum_i (\beta_{iiz} + \beta_{izi} + \beta_{zii}) \; (i \text{ from } x \text{ to } z) \qquad (11)$$

and average value of second order hyperpolarizability (Kurtz et al., 1990) is:

$$< \gamma > = \frac{1}{5} \Big[\gamma_{xxxx} + \gamma_{yyyy} + \gamma_{zzzz} + 2 \left[\gamma_{xxyy} + \gamma_{yyzz} + \gamma_{xxzz} \right] \Big] \qquad (12)$$

From **Table 3** the changes in the NLO properties were observed after the introduction of different electron donating and withdrawing groups into **OP** framework. For the neutral forms I–V, β and γ values decrease in the order IV > III > V > II > I. For the assorted R groups, the thiophene group is a strong electron-donating group and the cyano is a strong electron withdrawing group and from the values in **Table 3** it is concluded that the introduction of a strong electron-donating group into OP is favorable for improving NLO responses. This is attributed to increase in electron density of the OP framework resulting in enhancement in induced ring current. However, introducing an electron withdrawing group like CN, enhances the NLO properties still as compared to OP-I but to a lesser extent. This unexpected NLO response of OP-V implies that the charge transfer pattern of OP-V is polydirectional in comparison with the OP-I. The calculated values of α and β for the studied OP dertivative were found close to Bianthraquinodimethane Modified [16]Annulene (Torrent-Sucarrat et al., 2011). So as to achieve more insight into NLO response of OP derivatives, we correlated two level model with first and second order hyperpolarizability of these derivatives. Oudar and Chemla by employing complex sum over states (SOS) expression established a simple link between β and low-lying charge-transfer transition through the two-level model (Oudar and Chemla, 1977). According to this model the static first hyperpolarizability is expressed by the following expression:

$$\beta \propto (\mu_{ee} - \mu_{gg}) \frac{\mu_{ge}^2}{E_{ge}^2} \qquad (13)$$

where μ_{ee} and μ_{gg} are the ground state and excited-state dipole moment, μ_{ge} is the transition dipole, and E_{ge} is the transition energy.

As seen in **Table 3** the improvement in β values with increasing electron donating abilities can be attributed to the increasing μ_{ge} and decreasing E_{ge} values. The result shows that the μ_{ge}^2 / E_{ge}^2 values of OP derivatives follow the trend IV > V > III > II > 1 and is in agreement with the β

as well as γ values except in case of OP-V. On comparing the OP-V (cyano substituted molecule) with OP-III (phenyl substituted molecules), it is found that OP-III compound possess smaller μ_{ge}^2 value. However, the static hyperpolarizability of the **OP-III** is higher than that of the cyano substituted molecule. The second order hyperpolarizabilities of **OP-II** and **OP-V** do not differ much instead of huge differences in their first order hyperpolarizabilities. Additionally, there is a good correlation between the hyperpolarizabilities and the BLA values on changing the donor groups. The trend for the hyperpolarizabilities and BLA values is OP-I < OP-II < OP-III < OP-V < OP-IV and OP-I > OP-II > OP-III < OP-V < OP-IV respectively. Thus, the acceptor group has little effect on the BLA value and does not contribute much to the change in hyperpolarizabilities. However, changing the donor groups has a better effect on the BLA value and the hyperpolarizabilities of these systems. Thus, our investigation has shown that substitution with electron withdrawing group like cyano enhances the n-type ability of **OP**, however the substitution with electron donating group like thiophene multiplies the NLO response of octaphyrins.

CONCLUSIONS

The charge transport and nonlinear performance of octaphyrin derivatives have been studied using DFT level of theory. Computationally calculated properties like electron affinity and ionization energy values show that all these derivatives are stable toward oxygen and water in the air. The reorganization energy values show that these octaphyrin derivatives are effective as n-type materials. The low lying orbital energy levels signify that OP derivatives show high oxidation and reduction stabilities. Nonlinear response of these derivatives was quantified in terms of polarizability and hyperpolarizability values. Understanding the above carried computational studies, it is concluded that the n-type material character enhances by introduction of electron withdrawing groups but the nonlinear response is solely increased by electron donating groups.

AUTHOR CONTRIBUTIONS

The work is designed and done by NI. IL assists in doing the calculations.

REFERENCES

Ahn, T. K., Kwon, J. H., Kim, D. Y., Cho, D. W., Jeong, D. H., Kim, S. K., et al. (2005). Comparative photophysics of [26]- and [28]hexaphyrins(1.1.1.1.1.1): large two-photon absorption cross section of aromatic [26]hexaphyrins(1.1.1.1.1.1). *J. Am. Chem. Soc.* 127, 12856–12861. doi: 10.1021/ja050895l

Alonso, M., Geerlings, P., and Proft, F. D. (2014). Exploring the structure–aromaticity relationship in Hückel and Möbius N-fused pentaphyrins using DFT. *Phys. Chem. Chem. Phys.* 16, 14396–14407. doi: 10.1039/C3CP55509G

Alonso, M., Geerlings, P., and De Proft, F. (2013). Topology switching in [32]heptaphyrins controlled by solvent, protonation, and *meso* substituents. *Chem. Eur. J.* 19, 1617–1628. doi: 10.1002/chem.201203295

Alyar, H., Kantarci, Z., Bahat, M., and Kasap, E. (2007). Investigation of torsional barriers and nonlinear optical (NLO) properties of phenyltriazines. *J. Mol. Struc.* 836, 516–520. doi: 10.1016/j.molstruc.2006.11.066

Anaka, Y., Mori, H., Koide, T., Yorimitsu, H., Aratani, N., and Osuka, A. (2011). Rearrangements of a [36]octaphyrin triggered by nickel(II) metalation: metamorphosis to a directly meso-β-linked diporphyrin. *Angew. Chem. Int. Ed.* 50, 11460–11464. doi: 10.1002/anie.201105809

Anguera, G., Kauffmann, B., Borrell, J. I., Borros, S., Sanchez-Garc, D., (2015). Quaterpyrroles as building blocks for the synthesis of expanded porphyrins. *Org. Lett.* 17, 2194–2197. doi: 10.1021/acs.orglett.5b00767

Cavaleiro, J. A. S., Neves, M. G. P. M. S., and Tome, A. C. (2003). Cycloaddition reactions of porphyrins. *ArkiVoc xiv* 2003, 107–130. doi: 10.3998/ark.5550190.0004.e11

Chandrashekar, T. K., and Venkatraman, S. (2003). Core-modified expanded porphyrins: new generation organic materials. *Acc. Chem. Res.* 36, 676–691. doi: 10.1021/ar020284n

Chang, Y. C., Kuo, M. Y., Chen, C. P., Lu, H. F., and Chao, I. (2010). On the air stability of n-channel organic field-effect transistors: a theoretical study of adiabatic electron affinities of organic semiconductors. *J. Phys. Chem. C* 114, 11595–11061. doi: 10.1021/jp1025625

Charrière, R., Jenny, T. A., Rexhausen, H., and Gossauer, A. (1993). The chemistry of polyphyrins 2. Syntheses of hexaphyrins and their metal complexes. *Heterocycles* 36, 1561–1575. doi: 10.3987/COM-93-6339

Cheng, Y. C., Silbey, R. J., da Siva Filho, D. A., Calbert, J. P., Cornil, J., and Bre'das, J. L. (2003). Three-dimensional band structure and bandlike mobility in oligoacene single crystals: a theoretical investigation. *J. Chem. Phys.* 118, 3764. doi: 10.1063/1.1539090

Dadsetani, M., and Omidi, A. R. (2015). A DFT study of linear and nonlinear optical properties of 2-methyl-4-nitroaniline and 2-amino-4-nitroaniline crystals. *J. Phys. Chem. C* 119, 16263–16275. doi: 10.1021/acs.jpcc.5b05408

Dai, Y., Li, Z., and Yang, J. (2014). Density functional study of nonlinear optical properties of grossly warped nanographene C80H30. *J. Phys. Chem. C* 118, 3313–3318. doi: 10.1021/jp409899n

Datta, A., and Pati, S. K. (2006). Dipolar interactions and hydrogen bonding in supramolecular aggregates: understanding cooperative phenomena for 1st hyperpolarizability. *Chem. Soc. Rev.* 35, 1305. doi: 10.1039/b605478a

Ditchfield, R., Hehre, W. J., and Pople, J. A. (1971). Self-consistent molecular-orbital methods. IX. An extended gaussian-type basis for molecular-orbital studies of organic molecules. *J. Chem. Phys.* 54, 724. doi: 10.1063/1.1674902

Fan, D., Yi, Y., Li, Z., Liu, W., Peng, Q., and Shuai, Z. (2015). Solvent effects on the optical spectra and excited-state decay of triphenylamine-thiadiazole with hybridized local excitation and intramolecular charge transfer. *J. Phys. Chem. A* 119, 5233–5240. doi: 10.1021/jp5099409

Fink, R., Heischkel, Y., Thelakkat, M., and Schmidt, H.-W. (1998). Synthesis and application of dimeric 1, 3, 5-triazine ethers as hole-blocking materials in electroluminescent devices. *Chem. Mater.* 10, 3620–3625. doi: 10.1021/cm980369b

Flemming, J., and Dolphin, D. (2002). Carbonyl ylide 1,3-dipolar cycloadditions with porphyrins. *Tetrahedron Lett.* 43, 7281–7283. doi: 10.1016/S0040-4039(02)01619-2

Franck, B., and Nonn, A. (1995). Novel porphyrinoids for chemistry and medicine by biomimetic syntheses. *Angew. Chem. Int. Ed. Engl.* 34, 1795–1811. doi: 10.1002/anie.199517951

Frisch, M. J., Trucks, G. W., Schlegel, H. B., Scuseria, G. E., Robb, M. A., Cheeseman, J. R., et al. (2009). *Gaussian 09, Revision D.01.* Wallingford CT: Gaussian, Inc.

Fu, Y., Shen, W., and Li, M. (2008). Geometries and electronic structures of co-oligomers and co-polymers based on tricyclic nonclassical thiophene: a theoretical study. *Macromol. Theory Simul.* 17, 385–392. doi: 10.1002/mats.200800041

Geffroy, B., Roy, P., and Prat, C. (2006). Organic light-emitting diode (OLED) technology: materials, devices and display technologies. *Polym. Int.* 55, 572–582. doi: 10.1002/pi.1974

Harriman, A., Maiya, B. G., Murai, T., Hemmi, G., Sessler, J. L., and Mallouk, T. E. (1989). Metallotexaphyrins: a new family of photosensitisers for efficient

generation of singlet oxygen. *J. Chem. Soc. Chem. Commun.* 314–316. doi: 10.1039/c39890000314

Hata, H., Kamimura, Y., Shinokubo, H., and Osuka, A. (2006). Synthesis of pyrrolidine-fused [34]- and [36]octaphyrins via 1,3-dipolar cycloaddition. *Org. Lett.* 8, 1169–1172. doi: 10.1021/ol060067c

Hiroto, S., Shinokubo, H., and Osuka, A. (2006). Porphyrin synthesis in water provides new expanded porphyrins with direct bipyrrole linkages: isolation and characterization of two heptaphyrins. *J. Am. Chem. Soc.* 128, 6568–6569. doi: 10.1021/ja061621g

Islam, N., and Chimni, S. S. (2017). DFT investigation on nonlinear optical (NLO) properties of novel borazine derivatives. *J. Mol. Strut.* 1130, 781. doi: 10.1016/j.molstruc.2016.10.100

Islam, N., Niaz, S., Manzoor, T., and Pandith, A. H. (2014). Theoretical investigations into spectral and non-linear optical properties of brucine and strychnine using density functional theory. *Spectrochim. Acta A* 131, 461–470. doi: 10.1016/j.saa.2014.04.089

Islam, N., and Pandith, A. H. (2014a). Analysis of vibrational spectra (FTIR and VCD) and nonlinear optical properties of $[Ru(L)_3]^{2+}$ complexes. *J. Coord. Chem.* 67, 3288–3310. doi: 10.1080/00958972.2014.961921

Islam, N., and Pandith, A. H. (2014b). Optoelectronic and nonlinear optical properties of triarylamine helicenes: a DFT study. *J. Mol. Model.* 20, 2535. doi: 10.1007/s00894-014-2535-7

Jasat, A., and Dolphin, D. (1997). Expanded porphyrins and their heterologs. *Chem. Rev.* 97, 2267–2340. doi: 10.1021/cr950078b

Jin, R., and Tang, S. (2013). Rational design of organoboron derivatives as chemosensors for fluoride and cyanide anions and charge transport and luminescent materials for organic light-emitting diodes. *J. Mol. Model.* 19, 1685–1693. doi: 10.1007/s00894-012-1734-3

Jurchescu, O. D., Baas, J., and Palstra, T. T. M. (2004). Effect of impurities on the mobility of single crystal pentacene. *Appl. Phys. Lett.* 84, 3061. doi: 10.1063/1.1704874

Kido, H., Shin, J. Y., and Shinokubo, H. (2013). Selective synthesis of a [32]octaphyrin(1.0.1.0.1.0.1.0) bis(palladium) complex by a metal-templated strategy. *Angew. Chem. Int. Ed.* 52, 13727–13730. doi: 10.1002/anie.201306905

Kim, J. Y., Yasuda, T., Yang, Y. S., and Adachi, C. (2013). Bifunctional star-burst amorphous molecular materials for OLEDs: achieving highly efficient solid-state luminescence and carrier transport induced by spontaneous molecular orientation. *Adv. Mater.* 25, 2666–2671. doi: 10.1002/adma.201204902

Kumar, R., Misra, R., Chandrashekar, T. K., Nag, A., Goswami, D., Suresh, E., et al. (2007). One-pot synthesis of core-modified rubyrin, octaphyrin, and dodecaphyrin: characterization and nonlinear optical properties. *Eur. J. Org. Chem.* 27, 4552–4562. doi: 10.1002/ejoc.200700466

Kurtz, H. A., Stewart, J. J. P., and Dieter, K. M. (1990). Calculation of the nonlinear optical properties of molecules. *J. Comput. Chem.* 11, 82–87. doi: 10.1002/jcc.540110110

Lakshmi, S., Dutta, S., and Pati, S. K. (2008). Molecular electronics: effect of external electric field. *J. Phy. Chem. C* 112, 14718–14730. doi: 10.1021/jp800187e

Latos-Grazynski, L. (2004). Bimetallic figure-eight octaphyrins split into four-pyrrolic macrocycles. *Angew. Chem. Int. Ed.* 43, 5124–5128. doi: 10.1002/anie.200460645

Lin, B. C., Cheng, C. P., and Lao, Z. P. (2003). Reorganization energies in the transports of holes and electrons in organic amines in organic electroluminescence studied by density functional theory. *J. Phys. Chem. A* 107, 5241–5251. doi: 10.1021/jp0304529

Lin, J., Sa, R., Zhang, M., and Wu, K. (2015). Exploring second-order nonlinear optical properties and switching ability of a series of dithienylethene-containing, cyclometalated platinum complexes: a theoretical investigation. *J. Phys. Chem. A* 119, 8174–8181. doi: 10.1021/acs.jpca.5b03456

Lin, T. Y., Chaudhari, A., and Lee, S. L. (2013). Correlation between substituent constants and hyperpolarizabilities for di-substituted trans-azobenzenes. *J. Mol. Model.* 19, 529–538. doi: 10.1007/s00894-012-1577-y

Liu, C. C., Mao, S. W., and Kuo, M. Y. (2010). Cyanated pentaceno[2,3-c]chalcogenophenes for potential application in air-stable ambipolar organic thin-film transistors. *J. Phys. Chem. C* 114, 22316–22321. doi: 10.1021/jp1099464

Liu, C. G., Su, Z. M., Guan, X. H., and Muhammad, S. (2011). Redox and photoisomerization switching the second-order nonlinear optical properties of

a tetrathiafulvalene derivative across six states: a DFT study. *J. Phys. Chem. C* 115, 23946–23954. doi: 10.1021/jp2049958

Liu, F., Yang, Y., Cong, S., Wang, H., Zhang, M., Bo, S., et al. (2014). Comparison of second-order nonlinear optical chromophores with D−π−A, D−A−π−A and D−D−π−A architectures: diverse NLO effects and interesting optical behaviour. *RSC Adv.* 4, 52991–52999. doi: 10.1039/C4RA08951K

Maiya, B. G., Harriman, A., Sessler, J. L., Hemmi, G., Murai, T., and Mallouk, T. E. (1989). Ground- and excited-state spectral and redox properties of cadmium(II) texaphyrin. *J. Phys. Chem.* 93, 8111–8115.

Marcos, E., Anglada, J. M., and Torrent-Sucarrat, M. (2014). Effect of the meso-substituent in the hückel-to-möbius topological switches. *J. Org. Chem.* 79, 5036–5046. doi: 10.1021/jo500569p

Marcus, R. A. (1957a). On the theory of oxidation-reduction reactions involving electron transfer. II. Applications to data on the rates of isotopic exchange reactions. *J. Chem. Phys.* 26, 867.

Marcus, R. A. (1957b). On the theory of oxidation-reduction reactions involving electron transfer. III. Applications to data on the rates of organic redox reactions. *J. Chem. Phys.* 26, 872.

Marder, M. R., Kippelen, B., Jen, A. K.-Y., and Peyghambarian, N. (1997). Design and synthesis of chromophores and polymers for electro-optic and photorefractive applications. *Nature* 388, 845–851.

McLean, A. D., and Chandler, G. S. (1980). Contracted gaussian basis sets for molecular calculations. I. Second row atoms, Z=11–18. *J. Chem. Phys.* 72, 5639.

Misra, R., and Chandrashekar, T. K. (2008). Structural diversity in expanded porphyrins. *Acc. Chem. Res.* 41, 265–279. doi: 10.1021/ar700091k

Misra, R., Kumar, R., Chandrashekar, T. K., Suresh, C. H., Nag, A., and Goswami, D. (2006). 22π smaragdyrin molecular conjugates with aromatic phenylacetylenes and ferrocenes: syntheses, electrochemical, and photonic properties. *J. Am. Chem. Soc.* 128, 16083–16091. doi: 10.1021/ja0628295

Mori, H., Aratani, N., and Osuka, A. (2012a). Synthesis of A2B6-type [36]octaphyrins: copper(II)-metalation-induced fragmentation reactions to porphyrins and N-fusion reactions of meso-(3-Thienyl) substituents. *Chem. Asian J.* 7, 1340–1346. doi: 10.1002/asia.201100919

Mori, H., Sung, Y. M., Lee, B. S., Kim, D., and Osuka, A. (2012b). Antiaromatic hexaphyrins and octaphyrins stabilized by the hydrogen-bonding interactions of meso-imidazolyl groups. *Angew. Chem. Int. Ed.* 51, 12459–12463. doi: 10.1002/anie.201207212

Naka, S., Okada, H., Onnagawa, H., Yamaguchi, Y., and Tsutsui, T. (2000). Carrier transport properties of organic materials for EL device operation. *Synth. Met.* 111, 331–333. doi: 10.1016/S0379-6779(99)00358-6

Naoda, K., and Osuka, A. (2014). Iridium complexes of [26]hexaphyrin(1.1.1.1.1.1) and [36]octaphyrin(1.1.1.1.1.1.1.1). *J. Porphyrins Phthalocyanines* 18, 652. doi: 10.1142/S1088424614500187

Newman, C. R., Frisbie, C. D., da Silva Filho, D. A., Brédas, J. L., Ewbank, P. C., and Mann, K. R. (2004). Introduction to organic thin film transistors and design of n-channel organic semiconductors. *Chem. Mater.* 16, 4436–4451. doi: 10.1021/cm049391x

O'Boyle, N. M., Tenderholt, A. L., and Langer, K. M. (2008). cclib: a library for package-independent computational chemistry algorithms. *J. Comp. Chem.* 29, 839–845. doi: 10.1002/jcc.20823

Oudar, J. L., and Chemla, D. S. (1977). Hyperpolarisabilities of the nitroanilines and their relations to the excited state dipole moment. *J. Chem. Phys.* 66, 2664–2668.

Pandith, A. H., and Islam, N. (2014). Electron transport and nonlinear optical properties of substituted aryldimesityl boranes: a DFT study. *PLoS ONE* 9:e114125. doi: 10.1371/journal.pone.0114125

Park, Y., Kim, B., Lee, C., Hyun, A., Jang, S., Lee, J. H., et al. (2011). Highly efficient new hole injection materials for OLEDs based on dimeric phenothiazine and phenoxazine derivatives. *J. Phys. Chem. C* 115, 4843–4850. doi: 10.1021/jp108719w

Pushpan, S. K., and Chandrashekar, T. K. (2002). Aromatic core-modified expanded porphyrinoids with meso-aryl substitutents. *Pure Appl. Chem.* 74, 2045–2055. doi: 10.1351/pac200274112045

Pushpan, S. K., Venkatraman, S., Anand, V. G., Sankar, J., Rath, H., and Chandrashekar, T. K. (2002). Inverted porphyrins and expanded porphyrins: an overview, proceedings - indian academy of sciences. *Chem. Sci.* 114, 311–338. doi: 10.1007/BF02703823

Rath, H., Sankar, J., PrabhuRaja, V., Chandrashekar, T. K., Joshi, B. S., and Roy, R. (2005b). Figure-eight aromatic core-modified octaphyrins with six meso links: syntheses and structural characterization. *Chem. Comm.* 26, 3343–3345. doi: 10.1039/b502327k

Rath, H., Sankar, J., Prabhu Raja, V., Chandrashekar, T. K., Nag, A., and Goswami, D. (2005a). Core-modified expanded porphyrins with large third-order nonlinear optical response. *J. Am. Chem. Soc.* 127, 11608–11609. doi: 10.1021/ja0537575

Rintoul, L., Harper, S. R., and Arnold, D. P. (2013). A systematic theoretical study of the electronic structures of porphyrin dimers: DFT and TD-DFT calculations on diporphyrins linked by ethane, ethene, ethyne, imine, and azo bridges. *Phys. Chem. Chem. Phys.* 15, 18951–18964. doi: 10.1039/c3cp53396d

Romain, M., Thiery, S., Shirinskaya, A., Declairieux, C., and Tondelier, D. (2015). ortho-, meta-, and para-dihydroindenofluorene derivatives as host materials for phosphorescent OLEDs. *Angew. Chem. Int. Ed.* 54, 1176–1180. doi: 10.1002/anie.201409479

Sajan, D., Joe, H., Jayakumar, V. S., and Zaleski, J. (2006). Structural and electronic contributions to hyperpolarizability in methyl p-hydroxy benzoate. *J. Mol. Struc.* 785, 43–53. doi: 10.1016/j.molstruc.2005.09.041

Sasabe, H., and Kido, J. (2011). Multifunctional materials in high-performance OLEDs: challenges for solid-state lighting. *Chem. Mater.* 23, 621–630. doi: 10.1021/cm1024052

Sasabe, H., and Kido, J. (2013a). Development of high performance OLEDs for general lighting. *J. Mater. Chem. C* 1, 1699–1707. doi: 10.1039/c2tc00584k

Sasabe, H., and Kido, J. (2013b). Recent progress in phosphorescent organic light-emitting devices. *Eur. J. Org. Chem.* 2013, 7653–7663. doi: 10.1002/ejoc.201300544

Sekine, C., Tsubata, Y., Yamada, T., and Kitano, M. (2014). Recent progress of high performance polymer OLED and OPV materials for organic printed electronics. *Sci. Technol. Adv. Mater.* 15:034203. doi: 10.1088/1468-6996/15/3/034203

Sessler, J. L., and Davis, J. M. (2001). Sapphyrins: versatile anion binding agents. *Acc. Chem. Res.* 34, 989–997. doi: 10.1021/ar980117g

Sessler, J. L., Gebauer, A., and Weghorn, S. J. (2000a). "Porphyrin isomers," in *The Porphyrin Handbook Expanded Porphyrins, Vol. 2*, ed K. M. Kadish (Academic Press: San Diego), 1–54.

Sessler, J. L., Gebauer, A., and Weghorn, S. J. (2000b). "Expanded porphyrins," in *Expanded Porphyrins, Vol. 2*, eds K. M. Kadish, K. M. Smith, and R. Guilard (San Diego, CA: Academic Press), 55–121.

Sessler, J. L., Mody, T. D., Hemmi, G. W., Lynch, V., Young, S. W., and Miller, R. A. (1993). Gadolinium(III) texaphyrin: a novel MRI contrast agent. *J. Am. Chem. Soc.* 115, 10368–10369. doi: 10.1021/ja00075a066

Shimizu, S., Tanaka, Y., Youfu, K., and Osuka, A. (2005). Dicopper and disilver complexes of octaphyrin(1.1.1.1.1.1.1.1): reversible hydrolytic cleavage of the pyrrolic ring to a keto–imine. *Angew. Chem. Int. Ed.* 44, 3726–3729. doi: 10.1002/anie.200500676

Shionoya, M., Furuta, H., Lynch, V., Harriman, A., and Sessler, J. L. (1992). Diprotonated sapphyrin: a fluoride selective halide anion receptor. *J. Am. Chem. Soc.* 114, 5714–5722. doi: 10.1021/ja00040a034

Silva, A. M. G., Tome, A. C., Neves, M. G. P. M. S., and Cavaleiro, J. A. S. (2002b). Porphyrins in 1,3-dipolar cycloaddition reactions: synthesis of a novel pyrazoline-fused chlorin and a pyrazole-fused porphyrin. *Synlett* 1155–1157. doi: 10.1055/s-2002-32581

Silva, A. M. G., Tome, A. C., Neves, M. G. P. M. S., Silva, A. M. S., Cavaleiro, J. A. S., and Dondoni, A. (2002a). Porphyrins in 1,3-dipolar cycloaddition reactions with sugar nitrones. Synthesis of glycoconjugated isoxazolidine-fused chlorins and bacteriochlorins. *Tetrahedron Lett.* 43, 603–605. doi: 10.1016/S0040-4039(01)02243-2

Sprutta, N., and Latos-Grazyński, L. (2001). Figure-eight tetrathiaoctaphyrin and dihydrotetrathiaoctaphyrin. *Chem. Eur. J.* 7, 5099–5112. doi: 10.1002/1521-3765(20011203)7:23<5099::AID-CHEM5099>3.0.CO;2-M

Sundaraganesan, N., Karpagam, J., Sebastian, S., and Cornard, J. P. (2009). The spectroscopic (FTIR, FT-IR gas phase and FT-Raman), first order hyperpolarizabilities, NMR analysis of 2,4-dichloroaniline by ab initio HF and density functional methods. *Spectrochim. Acta A* 73, 11–19. doi: 10.1016/j.saa.2009.01.007

Tanaka, T., and Osuka, A. (2016). Chemistry of meso-aryl-substituted expanded porphyrins: aromaticity and molecular twist. *Chem. Rev.* 117, 2584–2640. doi: 10.1021/acs.chemrev.6b00371

Tao, Y., Yang, C., and Qin, J. (2011). Organic host materials for phosphorescent organic light-emitting diodes. *Chem. Soc. Rev.* 40, 2943–2970. doi: 10.1039/c0cs00160k

Tavernier, H. L., and Fayer, M. D. (2000). Distance dependence of electron transfer in DNA: the role of the reorganization energy and free energy. *J. Phys. Chem. B* 104, 11541–11550. doi: 10.1021/jp001362w

Thanthiriwatte, K. S., and de Silva, K. M. N. (2002). Non-linear optical properties of novel fluorenyl derivatives—ab initio quantum chemical calculations. *J. Mol. Struct. THEOCHEM* 617, 169–175. doi: 10.1016/S0166-1280(02)00419-0

Torrent-Sucarrat, M., Anglada, J. M., and Luis, J. M. (2011). Evaluation of the nonlinear optical properties for annulenes with hückel and möbius topologies. *J. Chem. Theory Comput.* 7, 3935–3943. doi: 10.1021/ct2005424

Torrent-Sucarrat, M., Anglada, J. M., and Luis, J. M. (2012). Evaluation of the nonlinear optical properties for an expanded porphyrin Hückel-Möbius aromaticity switch. *J. Chem. Phys.* 137, 184306. doi: 10.1063/1.4765667

Usta, H., Risko, C., Wang, Z. M., Huang, H., Deliomeroglu, M. K., Zhukhovitskiy, A., et al. (2009). Design, synthesis, and characterization of ladder-type molecules and polymers. air-stable, solution-processable n-channel and ambipolar semiconductors for thin-film transistors via experiment and theory. *J. Am. Chem. Soc.* 131, 5586–5608. doi: 10.1021/ja809555c

Weghorn, J., Sessler, J. L., Lynch, V., Baumann, T. F., and Sibert, J. W. (1996). bis[(μ-chloro)copper(II)] amethyrin: a bimetallic copper(II) complex of an expanded porphyrin. *Inorg. Chem.* 35, 1089–1090. doi: 10.1021/ic9509692

Werner, A., Michels, M., Zander, L., Lex, J., and Vogel, E. (1999). A new method for the synthesis of nonsymmetrical sulfamides using burgess-type reagents. *Angew. Chem.* 111, 3866–3870.

Wu, T., Chou, H., Huang, P., Cheng, C., and Liu, R. (2014). 3,6,9,12-tetrasubstituted chrysenes: synthesis, photophysical properties, and application as blue fluorescent OLED. *J. Org. Chem.* 79, 267–274. doi: 10.1021/jo402429q

Yanai, T., Tew, D., and Handy, N. (2004). A new hybrid exchange–correlation functional using the Coulomb-attenuating method (CAM-B3LYP). *Chem. Phys. Lett.* 393, 51–57. doi: 10.1016/j.cplett.2004.06.011

Zhang, R., Du, B., Sun, G., and Sun, Y. (2010). Experimental and theoretical studies on o-, m- and p-chlorobenzylideneaminoantipyrines. *Spectrochim. Acta A* 75, 1115–1124. doi: 10.1016/j.saa.2009.12.067

Zhao, C., Ge, H., Yin, S., and Wang, W. (2014). Theoretical investigation on the crystal structures and electron transport properties of several nitrogen-rich pentacene derivatives. *J. Mol. Model.* 20, 2158. doi: 10.1007/s00894-014-2158-z

Zhou, W., Kuebler, S. M., Braun, K. L., Yu, T., Cammack, J. K., Ober, C. K., et al. (2002). An efficient two-photon-generated photoacid applied to positive-tone 3D microfabrication. *Science* 296, 1106–1109. doi: 10.1126/science.296.5570.1106